METABOLITE NULLING TO MEASURE THE MACROMOLECULE BASELINE FOR QUANTITATIVE ^{1}H MAGNETIC RESONANCE SPECTROSCOPY AT 7 TESLA

J. Penner[1,2], A. Curtis[1,2], M. Klassen[1], J. Gati[1], M. Smith[3], M. J. Borrie[3,4], and R. Bartha[1,2]

[1]Centre for Functional and Metabolic Mapping, Robarts Research Institute, London, ON, Canada, [2]Medical Biophysics, University of Western Ontario, London, ON, Canada, [3]Division of Aging, Rehabilitation, and Geriatric Care, Lawson Health Research Institute, London, ON, Canada, [4]Department of Medicine, University of Western Ontario, London, ON, Canada

Background: Metabolite levels measured by short echo-time proton (^{1}H) magnetic resonance spectroscopy (MRS) may provide indicators of disease progression in conditions such as Alzheimer disease (AD). The use of high magnetic fields (e.g. 7 Tesla (T)) increases signal to noise ratio and spectral dispersion leading to improved metabolite quantification. Metabolite level changes have been demonstrated in multiple brain regions in AD at lower fields, including within the hippocampus [1]. Furthermore, it has been postulated that these levels can be used to detect the early onset of AD and monitor treatment response. Short echo-time spectroscopy measurements must account for the broad macromolecule baseline [2], either by fitting [3], or by direct measurement and subtraction [4]. The purpose of this study was to determine the optimal inversion time (TI) at 7T to null metabolite signals allowing accurate measurement of the macromolecule baseline. Spectra were acquired using a single-voxel localization by adiabatic selective refocusing (LASER) sequence [4].

Method: A 7T Varian/Siemens MRI system with a 12 channel transmit and receive head coil (built in-house) was used to acquire single-voxel short echo-time ^{1}H MR spectra as previously described [5], from within a phantom. A LASER [4] sequence (TR/TE = 4500/41.2 ms) was used that consists of a global adiabatic half-passage excitation pulse (5.12 ms) followed by three pairs (one pair for each orthogonal dimension) of slice-selective adiabatic full-passage pulses (hyperbolic secant, R10, 5.14 ms). A non-selective 5.12 ms adiabatic full-passage pulse was also used for signal inversion. Eight global 5 ms gaussian pulses were used for variable pulse power and optimized relaxation delays (VAPOR) water suppression [6]. T_1-weighted gradient echo images were used for voxel placement (Figure 1). The phantom consisted of an aqueous center ball, surrounded by a ring of a white matter mimicking agarose gel, surrounded by a ring of gray matter mimicking agarose gel. The concentrations of metabolites within the center ball are listed in Table 1. The metabolite inversion times (TI) were arrayed from 0ms to 3000 ms as shown in Figure 3, to determine the T_1 values of N-acetylaspartate (NAA) and creatine (Cr) within the center ball. A representative spectrum is shown in Figure 2. The peak heights ($M_z(t)$) of each metabolite at 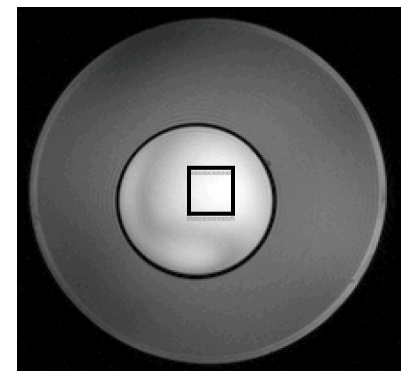each inversion time (t = TI) were fit to the longitudinal relaxation equation ($M_z(t) = M_o[1-\exp(-t/T_1)]$) to determine the T_1 values of NAA and Cr.

Figure 1: Transverse T1-weighted gradient echo image used for voxel placement (black box, 3cm^2, TE/TR = 3.1/6.2 ms)

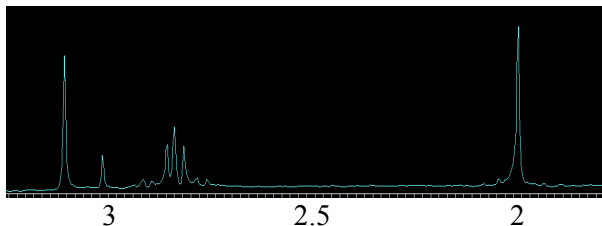Figure 2: NAA and Cr spectrum at TI of 3.165 seconds, with 1 Hz line broadening

Results and Discussion: The TI value that would theoretically result in complete suppression of NAA and Cr were found to be 0.47 seconds and 1.27 seconds, respectively. Furthermore, the T_1 values for NAA and Cr were found to be 1.28 seconds and 2.45 seconds, respectively (Table 1). The large difference in optimal inversion times between NAA and Cr suggests that multiple inversion pulses will be required to achieve adequate suppression for all metabolites. Future work will extend this method to determine the optimal TI values for in-vivo metabolite suppression.

Metabolite	Concentration (mM)	T_1 (s)	TI (s)
NAA	9.73	1.28 (CSF)	0.47 (CSF)
Cr	7.36	2.45 (CSF)	1.27 (CSF)

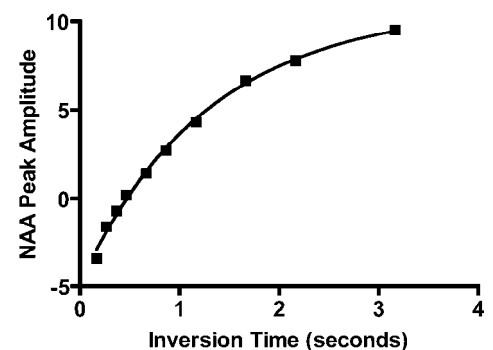Table 1: Phantom metabolite concentrations and measured T_1 and optimal TI values

Figure 3: NAA Inversion Recovery Curve

References:
[1] Block, W. et al., Arch of Neurology 59:828-834 (2002).
[2] Behar, K. L. et al., Magn Reson Med 32:294–302 (1994).
[3] Provencher, S. W. et al., Magn Reson Med 30:672–679 (1993).
[4] Garwood, M. et al., J Magn Reson 153:155-177 (2001).
[5] Kassem, M. et al., Magn Reson Med 49(5): 918-27 (2003).
[6] Tkac, I. et al., Magn Reson Med 41:649-656 (1999).